Soils and Rocks

An International Journal of Geotechnical and Geoenvironmental Engineering

www.soilsandrocks.com

ISSN 1980-9743
ISSN-e 2675-5475

The influence of the construction methodology on the modelled response of shafts

António M. G. Pedro[1#], David M. G. Taborda[2], Lucas M. Repsold[3], Jorge Almeida e Sousa[3]

Article

Keywords
Shaft excavation
Construction methods
Numerical modelling

Abstract

Shaft excavation is essential in modern cities, allowing for quick and direct access to the underground, where most transportation networks and utilities are being installed to reduce surface congestion. Selecting the appropriate construction methodology is critical to minimize ground movements, while ensuring structural stability and construction efficiency. This study assesses the performance of three typical construction methodologies – Excavation Before Support (EBS), Support Before Excavation (SBE) and Dual-Lined Shafts (DLS) – through a comprehensive numerical study. The validation of the adopted modelling approach for each methodology is performed by simulating three case studies in close proximity to each other. Several aspects of numerical modelling are discussed, such as the simulation of the hardening behavior of the sprayed concrete, the modelling the wall installation and their stiffness anisotropy. For each methodology, the influence of key variables is assessed through parametric studies, highlighting the importance of the excavation step height, the lining thickness and the embedded length of the wall. A final study, where all methodologies are compared for the same ground conditions, is carried out for two shaft diameters. Results indicate that SBE produces the smallest ground movements but induces the highest lining forces. In contrast, EBS originates higher ground movements due to significant soil decompression but smaller lining forces. DLS methodology exhibits an intermediate behavior, although more similar to that observed in EBS. These findings emphasize the importance of selecting an adequate shaft construction methodology and provide valuable information regarding the appropriate numerical simulation of each technique.

1. Introduction

The sustainable development of urban centers is directly interconnected with the exploration of their underground. Many cities are currently developing and implementing plans to minimize the impact of traffic congestion, lack of green spaces and affordable housing at ground surface by relocating and installing more efficient transportation networks and utilities in the subsurface (Admiraal & Cornaro, 2016; Bobylev, 2016; Lin et al., 2022; Debrock et al., 2023; Kuchler et al., 2024). Since the most effective way to access underground is through the construction of shafts it is unsurprising that several case studies reporting construction details and monitoring data have been published in recent years (Schwamb & Soga, 2015; Faustin et al., 2018; Walton et al., 2018; Quigg, 2019; Falco et al., 2022; Royston et al., 2022). In contrast with earlier developments, where the typical shape of the shafts was rectangular, the vast majority of recently constructed shafts have a circular or ellipsoid shape (Pedro et al., 2019). These configurations are more efficient, minimizing lining thickness, since it takes advantage of the circumferential soil arching developed during the excavation, while reducing the associated ground movements (Muramatsu & Abe, 1996). Excavation methodologies have also improved significantly, making the excavation and support operations more efficient and safe (Doig, 2012). According to Faustin et al. (2018), shaft excavation techniques can be divided into two main categories. In the Excavation Before Support (EBS) method, excavation is performed prior to the installation of the support, while the opposite occurs in the Support Before Excavation

[#]Corresponding author. E-mail address: amgpedro@dec.uc.pt
[1]Universidade de Coimbra, Institute for Sustainability and Innovation in Structural Engineering, Advanced Production and Intelligent Systems, Department of Civil Engineering, Coimbra, Portugal.
[2]Imperial College London, Department of Civil and Environmental Engineering, London, United Kingdom.
[3]Universidade de Coimbra, Department of Civil Engineering, Coimbra, Portugal.

Submitted on March 2, 2025; Final Acceptance on July 31, 2025; Discussion open until February 28, 2026.

Editor: Renato P. Cunha

https://doi.org/10.28927/SR.2025.004025

(SBE) category, with the excavation only being executed after the support is in place. Naturally, the adequate selection of the shaft excavation technique depends on different factors, including ground and groundwater conditions, the shaft purpose and its dimensions, and the vulnerability of the surrounding structures. As demonstrated by Pedro et al. (2024), the construction technique and even the type of lining employed can have a considerable impact in the carbon dioxide emissions associated with the shaft construction, raising issues associated with the need to evaluate the sustainability of the chosen solution during the design process.

The EBS technique resembles the sequential excavation of a tunnel but in the vertical direction. The soil is sequentially excavated in steps, typically of 1 to 1.5m in height, around the shaft perimeter followed by the installation of the lining, which typically consists of either pre-cast concrete segments (PCS) or sprayed concrete (SCL) (Gomes, 2008). In contrast, the SBE methodology involves pre-installation of the lining – typically diaphragm walls or bored piles – forming a circular retaining structure, after which the enclosed soil is excavated. The construction of shafts using jacked pre-cast segments is generally included within the SBE category, as the segments provide support before soil excavation (Faustin et al., 2018). However, to facilitate the jacking-in process, some soil is usually removed within the shaft causing its decompression. Depending on the amount of soil removed the technique can resemble either SBE (for minimal removal) or EBS (for significant removal). Faustin et al. (2018) also reported cases where both SBE and EBS methodologies were combined, termed dual-lined shafts (DLS). In these cases, the upper section of the shaft, where poorer materials were found, consisted of a diaphragm wall, while in the lower section the excavation followed a sequential approach with SCL applied.

Despite the significant differences between the shaft construction techniques, there is a lack of published studies assessing their relative impact, with most of the research focusing on evaluating the influence of shaft dimensions and soil properties on the ground deformations for a specific excavation technique (Schwamb & Soga, 2015; Le et al., 2019; Taborda et al., 2025b). The study performed by Pedro et al. (2024), although primarily focusing on evaluating the sustainability of construction methods, showed that in EBS the unsupported excavation caused considerable soil decompression, resulting in significant settlements and lateral wall movements. In contrast, in SBE, ground movements were smaller, and heave was inclusively measured at the top of the wall due to the soil decompression at the excavation base. Pedro et al. (2024) also observed that the pre-installed lining in SBE constrained the surrounding soil, leading to higher forces in the lining compared to those observed when adopting an EBS methodology. In the latter case, the forces acting on the lining were determined by the height of each excavation step, as pressures are transferred to the lining above and the soil beneath through the development of a vertical arching effect (Pedro et al., 2024; Repsold et al., 2024).

Through a comprehensive set of numerical analyses, this paper aims to compare the behavior of a shaft excavated employing three different construction sequences – EBS, SBE and DLS. The study compares key aspects of each methodology and evaluates their impact on the ground movements, pressures and forces acting on the lining. The validation of the numerical model is performed by comparing the modelled behavior against monitoring data gathered from three case studies, each employing one of these methodologies. In the validation process, various aspects related to the modelling procedures that are often neglected are analyzed in order to determine the most suitable approaches for simulating accurately each type of construction methodology.

2. Numerical modelling of shafts

2.1 General considerations

With the development of major tunnelling projects in London a large database was compiled on the construction of shafts using different techniques. Despite the differences in construction methods and shaft geometries the results presented by Faustin et al. (2018) show that a good performance was achieved in all cases. From these, three shafts were selected in this paper for analysis, each representing a distinct construction methodology, as they were all excavated in the same materials, reached similar depths, and had detailed information and measurements of settlements for the key excavation stages. The geometry and ground conditions at the three site locations are illustrated in Figure 1.

In the London Power Tunnels project, the EBS technique was used in the construction of the Channel Gate Road (CGR) shaft. This shaft had an outer diameter (D) of 13.1 m and reached a depth (H) of 32.9 m, with the upper 22.2 m supported by PCS with a thickness of 0.325 m, while, in lower part of the shaft, 0.312 m thick SCL was placed. The Whitechapel Cambridge Heath (WCH) shaft, built as part of the Crossrail project, had an outer diameter of 31.2 m and a depth of 32 m. The SBE technique was applied in this shaft, with the installation of a 1.5 m thick and 40.5 m deep diaphragm wall, before excavating the enclosed soil. In the Northern Line Extension project, Kennington Green (KG) shaft, with an outer diameter of 16.2 m and 26.1 m deep, was constructed using the DLS methodology. Initially, secant bored piles with a diameter of 0.60 m and a depth of 13.6 m were installed, followed by the excavation of the enclosed soil. In the second phase, the remaining soil was excavated sequentially in steps and 0.6 m thick SCL was applied along the contour of the excavation, following the traditional EBS approach. Faustin et al. (2018) also presented results of settlements induced by jacked shafts, but the information about the construction sequence was incomplete, preventing the simulation of its excavation without significant assumptions

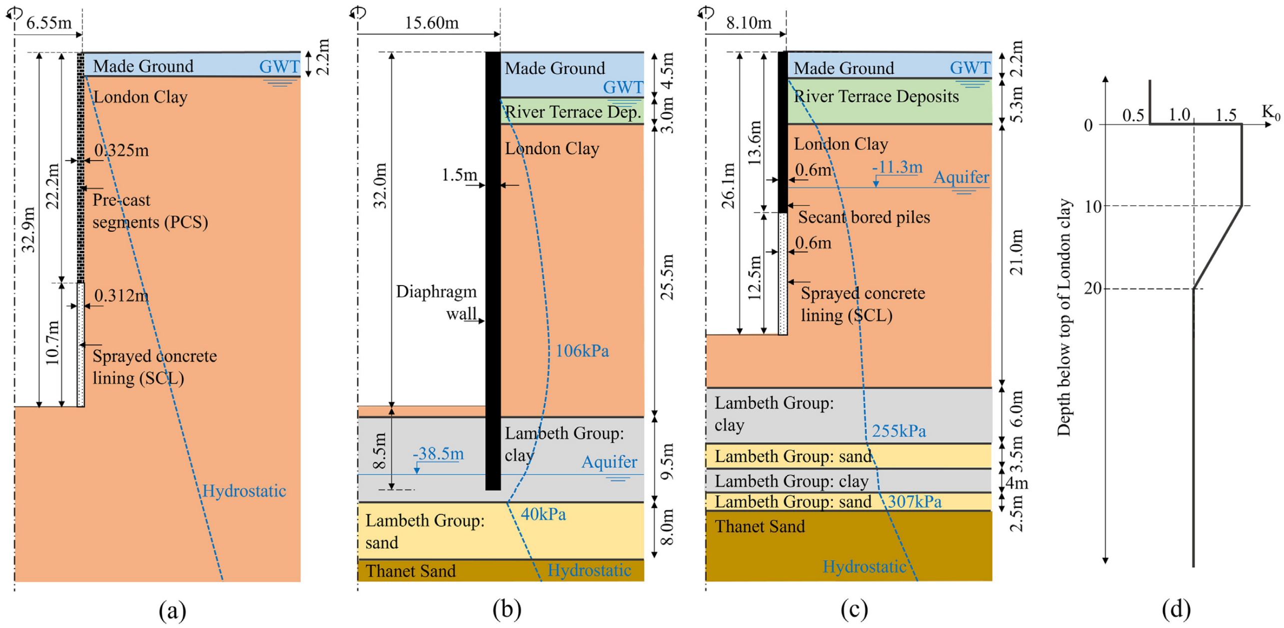

Figure 1. Geometry and ground conditions at the site locations: (a) CGR; (b) WCH; (c) KG; (d) K_0 profile.

that could impact the results. As a result, jacked shafts were excluded from this study.

At all three sites, variations of the typical ground conditions in London are found (King, 1981). At CGR, beneath a thin layer of Made Ground, there is a thick deposit of London Clay extending to more than 75 m. At WCH, the superficial deposits are thicker, with Made Ground and River Terrace Deposits having a combined thickness of 7.5 m. Below, a 25.5 m thick layer of London Clay is followed by Lambeth Group (17.5 m thick), with its typical interbedded clay and sand layers; at greater depths lies the Thanet Sand deposit (Crossrail Ltd., 2011). The stratigraphy at KG is similar to that of WCH, with slight differences in the thickness of layers. According to Schroeder et al. (2004) who considered a site in close proximity to the KG site, the Lambeth Group presents more frequent intercalations of sand and clay.

As discussed in Simpson et al. (1989), the groundwater profile in the London basin is typically underdrained, with various factors, including the thickness of the soil formations, the variation of permeability with depth and the location of the lower aquifer, affecting the pore water pressure distribution. At all sites the ground water table (GWT) was found at the bottom of the Made Ground. However, while at CGR a hydrostatic profile can be assumed, due to the significant thickness of London Clay, at the other two sites an underdrained profile is encountered. According to Crossrail Ltd. (2011), at WCH, the ground water pressure in the top of the sandy layer of the Lambeth Group is approximately 40 kPa, indicating that the aquifer level is located approximately 4 m above, at a depth of 38.5 m, while at KG, the aquifer is estimated at approximately 11.3 m depth (Schroeder et al. (2004)). By imposing these groundwater conditions, the pore water pressure distribution can be estimated through a steady-state analysis, assuming the variations with depth of permeability detailed in the subsequent section. The obtained distributions are represented in Figure 1, with WCH exhibiting a much more pronounced underdrainage, due to a significantly deeper lower aquifer. It should be noted that, prior to excavation dewatering was carried out through sumps or depressurization wells located within the shafts. According to Faustin et al. (2018), there was little drainage of groundwater associated with the shaft construction due to the low permeability of the formations, making settlements likely to be very small. Consequently, in this study, and in the absence of monitoring data, the settlements induced by prior dewatering were disregarded.

2.2 Details of the numerical analysis

The numerical simulations of the shafts excavation were performed using Plaxis 2D (Bentley Systems, 2024), with all analyses performed as coupled consolidated and making use of the axisymmetry of the problem. The top boundary corresponded to the ground surface and the left-hand size boundary to the axis of symmetry. To minimize the boundary effects, the right-hand side and bottom boundaries were positioned at distances of 100 m and 70 m, respectively. The water flow and the displacements in the horizontal direction were restricted in both lateral boundaries while along the bottom boundary no displacements were allowed. The domain was discretized in 15-noded triangular elements each with 12 Gaussian integration points for determining the displacements and stress states (Bentley Systems, 2024), respectively. 5-noded plate elements were also used in some of the models to simulate the shaft lining. In the zone around the shaft wall a higher concentration of elements was employed in order to capture the higher stress and strain variations expected in that zone. Lastly, 12-noded interface elements were placed between the lining and the retained soil to prevent water inflow and to simulate the soil-structure interaction. Figure 2 shows the detail around the shaft of the mesh employed in each of the case studies analyzed.

The initial conditions were generated assuming a geostatic profile, with the vertical total stresses determined based on a unit weight of 18 kN/m^3 for the Made Ground and 20 kN/m^3 for all other formations. The horizontal total stress was calculated using the at-rest coefficient of earth pressure (K_0) profile presented in Figure 1d, which replicates that adopted on previous studies (Gawecka et al., 2017; Sailer et al., 2019; Taborda et al., 2025b). As previously mentioned, the initial pore water pressure profile was obtained through a steady-state analysis, ensuring equilibrium based on the specified GWT and aquifer locations.

A linear elastic-perfectly plastic behavior was adopted for the Made Ground, with a stiffness characterized by E = 10 MPa and ν = 0.2 and its strength described by the Mohr-Coulomb failure criterion with ϕ' = 30º, c' = 0 kPa and ψ' = 0º (Taborda et al., 2025b). For the other formations the non-linear elastic-perfectly plastic IC MAGE M01 model, developed by Taborda et al. (2024a) and implemented into Plaxis 2D as a user-defined soil model, was employed, as it has been shown to effectively capture the complex behavior of these formations in different geotechnical applications (Gawecka et al., 2017; Sailer et al., 2019; Taborda et al., 2025b). In this model, strength is characterized by the Mohr-Coulomb failure criterion and the stiffness by non-linear elastic relationships for both the tangent shear and bulk moduli (Taborda et al., 2016). The specific implementation of the model for Plaxis User-Defined Soil Model is detailed in Taborda et al. (2024b). Table 1 presents the parameters employed in the analysis, which were adopted from the previous studies by Gawecka et al. (2017) and Sailer et al. (2019).

The Made-Ground was assumed to be dry since it was above GWT, while for the sandy materials (River Terrace Deposits, Lambeth Group: sand and Thanet Sand) a drained condition with an isotropic permeability of 1x10^{-5} m/s was adopted. For the London Clay and Lambeth Group: clay formations, an undrained condition was specified, with anisotropic permeability given by Equation 1:

$$\log_{10} k_v = 0.0215 \cdot \left(y - y_{LC}\right) - 9.427 \geq 1 \times 10^{-12} \left[m/s\right] \quad (1)$$

where k_v represents the vertical permeability, y is the vertical coordinate on the model and y_{LC} is the coordinate of the top of the London Clay. As suggested by Taborda et al. (2025b) an anisotropy ratio of 2.0 was adopted between the horizontal and vertical permeabilities (k_h = 2 k_v). This permeability model was introduced in Plaxis as a user-defined flow model (Bui et al., 2019) as detailed in Taborda et al. (2023).

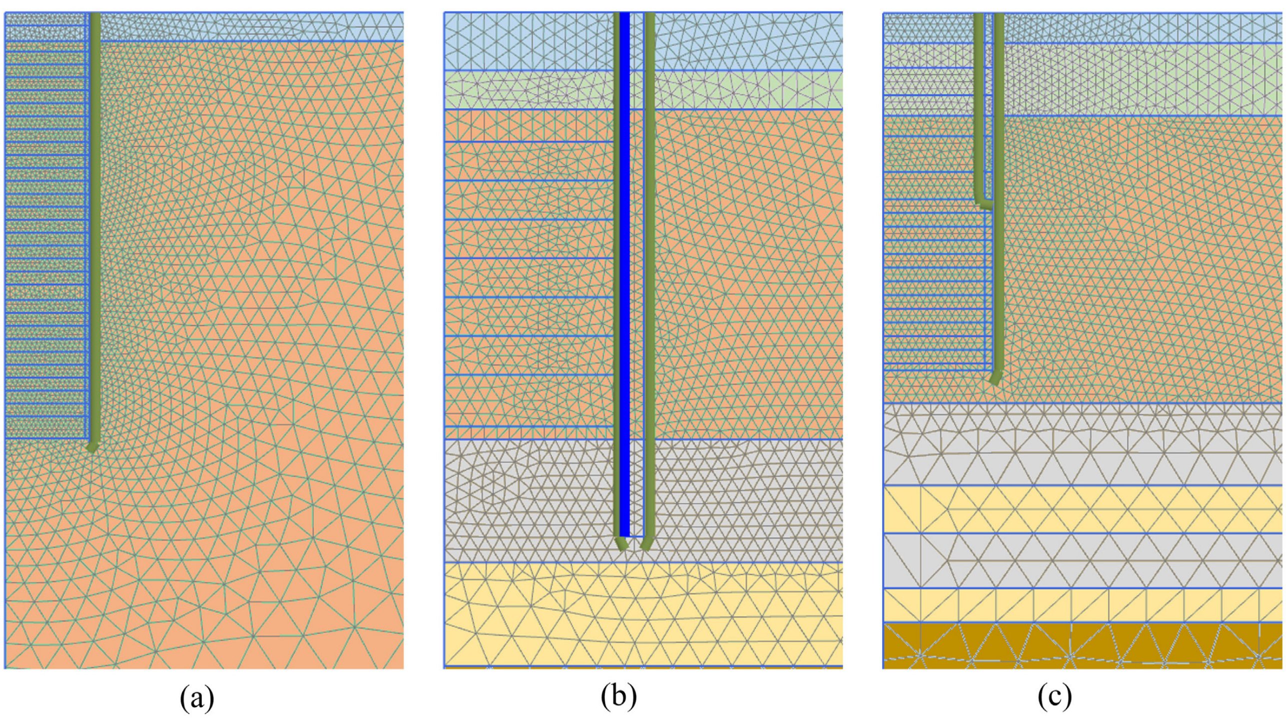

Figure 2. Detail around the shaft of the mesh employed in the numerical simulations: (a) CGR; (b) WCH; (c) KG.

Table 1. Parameters of the soils adopted in the analyses.

Parameter	River Terrace Deposits	London Clay	Lambeth Group: clay	Lambeth Group: sand	Thanet Sand
p'_{ref}	100.0	100.0	100.0	100.0	100.0
f' (°)	35.0	25.0	27.0	34.0	40.0
c' (kPa)	0.0	5.0	25.0	0.0	0.0
y' (°)	17.5	12.5	13.5	17.0	20.0
G_{ref} (kPa)	41939.61	51743.11	51924.52	81346.31	65275.23
m_G	1.0	1.0	1.0	1.0	1.0
a	0.000145	0.000056	0.000110	0.000015	0.000046
b	1.00	0.90	0.95	1.00	0.85
$R_{G,min}$	0.03511	0.06450	0.04662	0.14557	0.02631
G_{min}	3000.0	2667.0	2667.0	1000.0	2000.0
K_{ref} (kPa)	49843.08	26692.73	61331.71	49843.08	29813.53
m_K	1.0	1.0	1.0	1.0	1.0
r	0.000247	0.000127	0.000065	0.000026	0.000155
s	1.25	1.80	1.40	0.90	1.10
$R_{K,min}$	0.15440	0.13275	0.07589	0.08377	0.27947
K_{min}	3000.0	5000.0	5000.0	5000.0	5000.0

For modelling the lining of the shafts, four additional materials were required. For the PCS, diaphragm wall and bored piles a linear elastic behavior with the parameters presented in Table 2 was adopted.

Table 2. Parameters of the linings adopted in the analyses.

Parameter	PCS	Diaphragm wall	Bored piles
γ (kN/m^3)	25.0	25.0	25.0
E (GPa)	37.0	30.0	30.0
n	0.2	0.2	0.2

To describe the behavior of SCL, a non-linear time-dependent model was employed. The model IC MAGE M07 was implemented into Plaxis as a user-defined soil model (Taborda et al., 2025a) and is based on the Model Code 90 proposed by CEB-FIP (1993), where the stiffness is defined by Equation 2:

$$E\left(t_{conc}\right)=\sqrt{\exp\left[s\cdot(1-\left(\frac{28}{t_{conc}/1day}\right)^{1/2}\right]}\cdot E_{28} \tag{2}$$

where E_{28} is the stiffness of the material at 28 days, t_{conc} [days] is the age of the concrete and s is a parameter which depends on the type of concrete. In this study values of E_{28} = 30 GPa and s = 0.25 were used, together with v = 0.2.

Lastly, for the interface elements, a strength reduced to two-thirds of that of the adjacent soil was adopted, while the normal and tangential stiffnesses were set to 10^6 kN/m^3, in agreement with the values adopted by previous studies (Pedro et al., 2024; Taborda et al., 2025b).

2.3 Channel Gate Road shaft (CGR)

The numerical simulation of the CGR shaft followed the typical EBS sequence as described in Taborda et al. (2025b). After the generation of the initial pressures, the shaft was excavated and supported in 33 stages. In each stage, 1 m of soil was excavated, and the lining of the precedent excavation step was installed. This procedure was followed in all stages, except for the first two, which corresponded to the excavation of the Made Ground, where the excavation and support were performed simultaneously to avoid soil collapse, and in the last stage, where only the final piece of lining was installed. As illustrated in Figure 1, the upper part the shaft was supported by underpinned PCSs, while SCL was used in the lower part. An excavation rate of 1 m/day was adopted in all analyses, resulting in a total simulated duration of 32.9 days. To evaluate the influence of SCL hardening, two analyses were performed in which a constant value of 15 and 37 GPa were adopted for the Young's modulus of the SCL. The lower value represents the stiffness after about 1 day, according to Model Code 90 (CEB-FIP, 1993), while the higher value corresponds to a support stiffness equivalent to PCSs. Since the simulation of the lining is often performed using plate elements instead of solid elements, two additional analyses were carried out (B-E = 15 GPa; B-E = 37 GPa), each with a constant stiffness of 15 and 37 GPa, to evaluate the influence of using this type of element, instead of the solid elements used in the original analyses.

The final settlements (S_v) normalized by CGR shaft depth (H) are plotted in Figure 3 against the normalized distance behind the wall (x/H) for the five analyses performed. The results show that including SCL hardening leads to a better agreement with shaft monitoring data, particularly for the data located nearer to the shaft wall. At greater distances the model overestimates settlements and fails to reproduce the slight heave recorded on site. The effect of SCL hardening cannot be captured by using a constant Young's modulus, with even the analyses with the lower stiffness (15 GPa) predicting smaller settlements. The results also show that the difference between adopting the two extreme values of stiffness for solid elements is small, with the analysis where $E = 37$ GPa showing only slightly smaller settlements. Interestingly, when plate elements are used the impact of stiffness increases, leading to larger differences in settlements between the two stiffnesses considered. These results emphasize the importance of considering lining hardening in the modelling, which can only be accounted for using solid elements.

2.4 Whitechapel Cambridge Heath shaft (WCH)

Modeling the SBE methodology is apparently simpler, as it requires fewer stages compared to EBS methodology. After generating the initial stresses, the lining is installed, followed by the excavation of the enclosed soil until the shaft reaches its final depth. This approach was generally adopted in the excavation of WCH shaft, with the excavation of the soil carried out over 10 stages. One aspect that is often disregarded in SBE simulation is the installation of the lining, with most studies considering it simply as wished-in-place (WIP). However, for the WCH shaft, data regarding the installation of the diaphragm wall was available (Faustin et al., 2018), allowing for an assessment of its impact on the final settlements. As acknowledged in different studies there is some uncertainty in the simulation of the wall installation, particularly for deep walls, as the pressure of the wet concrete is not linearly distributed with depth (Lings et al., 1994; Gourvenec & Powrie, 1999). The numerical simulation of the wall installation was performed in three stages, as proposed by Schwamb & Soga (2015): (1) the panel was excavated and a pressure was applied in the contour of the excavation to simulate the presence of the bentonite (linearly increasing with depth, based on $g = 11$ kN/m^3); (2) an additional pressure representing wet concrete ($g = 25$ kN/m^3) was applied with its distribution with depth following that proposed in Gourvenec & Powrie (1999); (3) finally, the elements of the diaphragm wall and interface were activated and the boundary between them and the soil set to impermeable. Following the observation related to the importance of modelling concrete hardening when analysing the CGR shaft, model IC MAGE M07 was used to simulate the diaphragm wall material. It was assumed that the installation of the diaphragm wall took 1 day, followed by a rest period of 27 days to allow the concrete to cure before shaft excavation began. Since an excavation rate of 1 m/day was also adopted, a total duration of 60 days was simulated.

Several studies (Cabarkapa et al., 2003; Zdravkovic et al., 2005; Schwamb & Soga, 2015) have highlighted the importance of appropriately modelling wall stiffness in the circumferential direction, as the presence of joints between the diaphragm panels limits the development of hoop stiffness. In the absence of studies quantifying the anisotropy ratio between the vertical and circumferential stiffnesses (E_z/E_q), those studies tested different ratios and observed a significant increase in ground movements as the stiffness anisotropy ratio increases or, equivalently, as the circumferential stiffness reduces. To evaluate the importance of this aspect several analyses were performed with different stiffness anisotropy ratios.

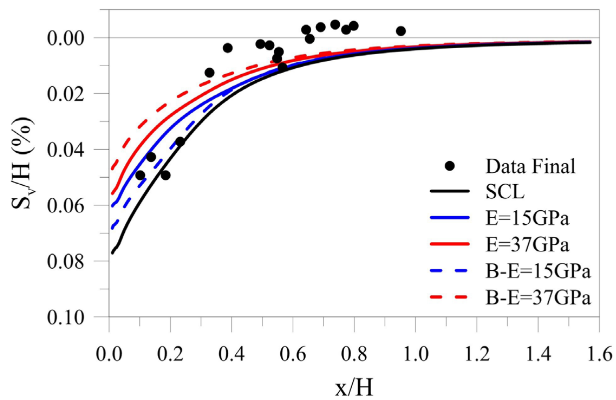

Figure 3. Settlements determined for CGR shaft.

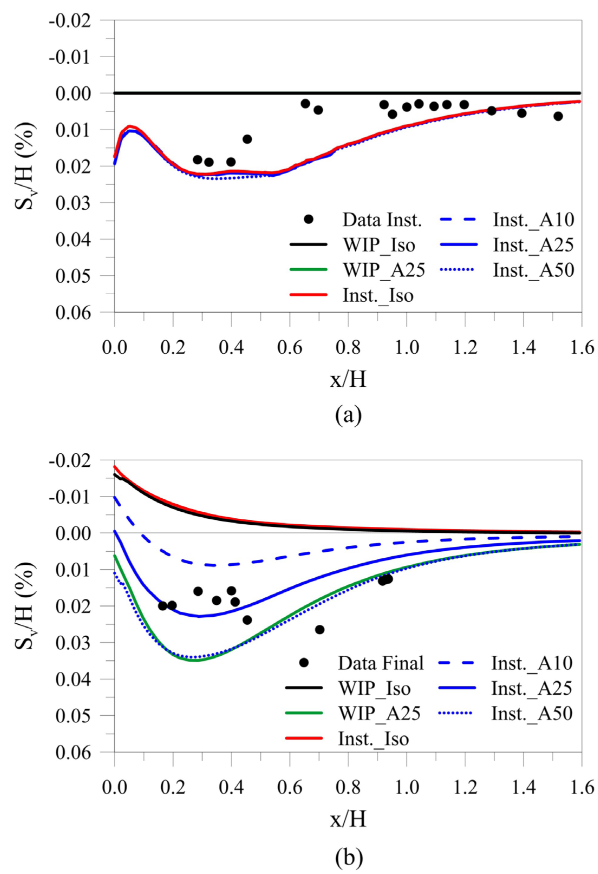

Figure 4. Settlements determined for WCH shaft: (a) Installation; (b) Final excavation.

Figure 4 illustrates the settlements induced by the diaphragm wall installation and those caused solely by shaft excavation (i.e. zeroed after the rest stage). As expected, no movements are obtained when the diaphragm wall is considered WIP. However, when the installation is simulated a reasonable agreement with the monitoring data is obtained, with the calculations slightly overestimating the maximum settlement and predicting a wider settlement trough. The differences between the analyses with different stiffness anisotropy ratios are negligible, with all analyses yielding identical results. In contrast, the predicted settlements due to the shaft excavation are strongly influenced by the stiffness anisotropy ratio. When an isotropic behavior is adopted (anisotropy ratio of 1) only heave is predicted, with its maximum value at the shaft wall and gradually decreasing with distance. As the stiffness anisotropy ratio increases to 10 (Inst._A10) or 50 (Inst._A50), settlements occur, reaching a maximum at a normalized distance of about 0.3 in all cases. Near the wall, the settlements are smaller and affected by its presence, due to the upward movements caused by the soil decompression at the base of the excavation. For the specific case of the WCH shaft, a stiffness anisotropy ratio of E_z/E_q=25 (Inst._A25) provides the best agreement with monitoring data. It is interesting to note that if WIP is adopted, there is no difference in settlements if isotropic behavior is adopted, but the best fitting stiffness anisotropy ratio is lower than 25, indicating that neglecting installation effects could impact the choice of affects the parameter selection. The influence of the stiffness anisotropy ratio is highlighted in Figure 5, where the maximum normalized settlement is plotted for several ratios tested, ranging from 1 (isotropic) to a 100. The results show that heave only occurs under isotropic behavior, while the maximum settlements increase almost linearly with the increase of the stiffness anisotropy ratio.

2.5 Kennington Green shaft (KG)

The DLS methodology adopted in the KG shaft combines both SBE and EBS techniques and, consequently, the simulation of its excavation followed the principles described in the previous sections. As a result, the bored piles were installed first, followed by soil excavation over 7 stages until the tip of the piles was reached. Subsequentially, excavation proceeded similarly to the CGR shaft where, in each stage, 1 m of soil was excavated, and the lining of the preceding excavation step was installed until the shaft reached its final depth. Similar to the previous case studies, additional analyses, following the

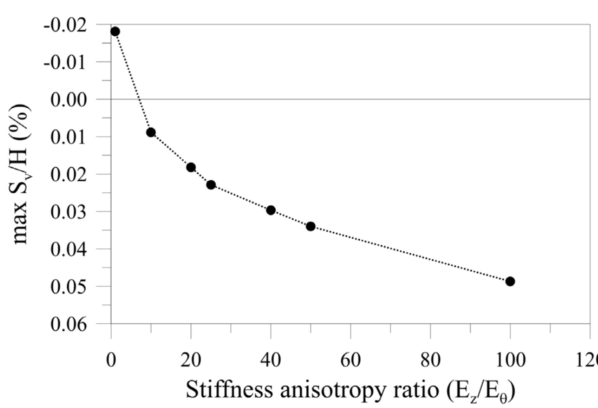

Figure 5. Influence of the stiffness anisotropy ratio in the maximum settlements determined for WCH shaft.

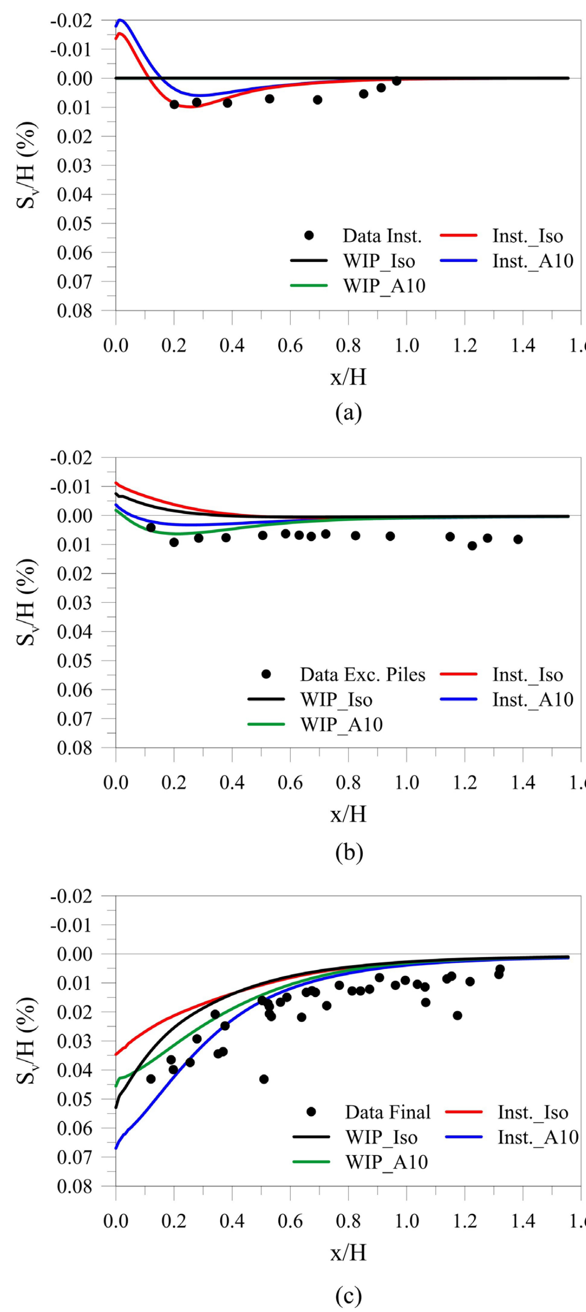

Figure 6. Settlements determined for KG shaft: (a) Installation; (b) Excavation of piles; (c) Final excavation.

same procedures applied for the WCH shaft, were performed to assess the effect of pile installation and stiffness anisotropy.

Figure 6 presents the settlements induced by the bored piles installation and those caused solely by shaft excavation (i.e. zeroed after the rest stage) for the stages where the tip of the piles is reached (end of SBE technique) and when full excavation is completed. A stiffness anisotropy ratio of 10 for the secant pile wall portion of the lining provided the best fit to the monitoring data across all stages. The installation of the bored piles induced very small settlements (less than 0.01%), which are slightly better predicted when an isotropic behavior of the lining was adopted. When the excavation reached the tip of the piles minimal settlements were also observed. Similar to the WCH shaft, an isotropic behavior resulted in heave at this stage, and only by introducing stiffness anisotropy was it possible to predict reasonably the measured settlements. At the final excavation stage, the settlements increased considerably, with the best prediction achieved when the installation of piles is considered and a stiffness anisotropy ratio of 10 is adopted, although the model predicts a slightly narrower settlement trough than that observed at the site.

3. Factors affecting the construction methodologies

Using the calibrated models as reference, a parametric study was carried out to evaluate the influence of key parameters for each methodology. The analysis focused on assessing the impact on ground movements, pressures and forces in the linings by varying parameters such as lining thickness, excavation step and length of the embedded wall.

3.1 EBS – Excavation Before Support

One of the main drawbacks of the EBS methodology is the high number of excavation-support cycles, which increase both cost and construction time. One option to minimize this issue is to increase the excavation step height. To evaluate the impact of such approach, additional analyses were performed using a 2 m height excavation step (double the height used in the reference CGR analysis). Another key aspect is the thickness of the lining (t), which varies significantly from case to case (Faustin et al., 2018), even under similar ground conditions and shaft geometries. This aspect was analyzed by increasing the lining thickness (PCS+SCL) to 0.600 m. A final analysis was performed in which the entire lining, except for the initial 2.2 m excavated on Made Ground, consisted of SCL, replacing the PCS employed in the upper part of the shaft, to assess if this aspect has a significant influence on the shaft behavior.

The settlements and the primary results for the lining are presented in Figures 7 and 8, respectively, for all additional analyses performed. As expected, increasing the excavation step to 2 m height induces higher settlements due to the greater soil decompression, with the maximum settlement near the wall increasing by about 25%. The influence of this aspect is also observed when the lining thickness is increased from 0.325 to 0.600 m, though in this case, the maximum settlement increase is only of approximately 19%. Interestingly, increasing the lining thickness and, consequently its stiffness, results in higher settlements rather than a decrease. This outcome is inherent to the EBS methodology and is justified by the greater weight of the lining. When a new excavation cycle begins, the lining is left hanging, with its weight acting as a destabilizing force, and naturally, a heavier lining leads to greater settlements. This effect is minimized on-site by adopting a construction sequence which involves several excavation steps in the circumferential direction rather than completing a full excavation cycle at once, though this approach increases considerably the number of operations required for shaft construction and cannot be reproduced numerically if axisymmetric conditions are assumed.

In all analyses, the horizontal displacements in the lining follow a similar pattern, increasing almost linearly with depth. The oscillations observed at each excavation step are a consequence of the EBS methodology, with the lower part of the lining installed at the previous step exhibiting higher displacements due to soil decompression and arching effect. Naturally, these oscillations and overall displacements increase with a larger excavation step height but are almost unaffected by the lining thickness. The total pressure acting on the lining is similar across all analyses, increasing almost linearly with depth until reaching the depth of the last excavation cycle, where it approaches zero due to the exposed soil surface. It should be noted that an averaging smoothing filter was applied to the total pressures results to remove the extremely high numerical stress concentrations that occur at excavation step transitions. These stress concentrations cause the fluctuations observed in the hoop forces within each excavation step height. On average, the hoop force tends to increase with depth, with smaller values

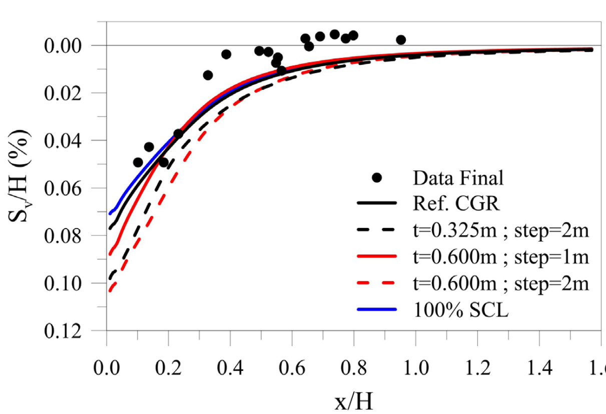

Figure 7. Influence of lining thickness and excavation step height on settlements in the EBS methodology.

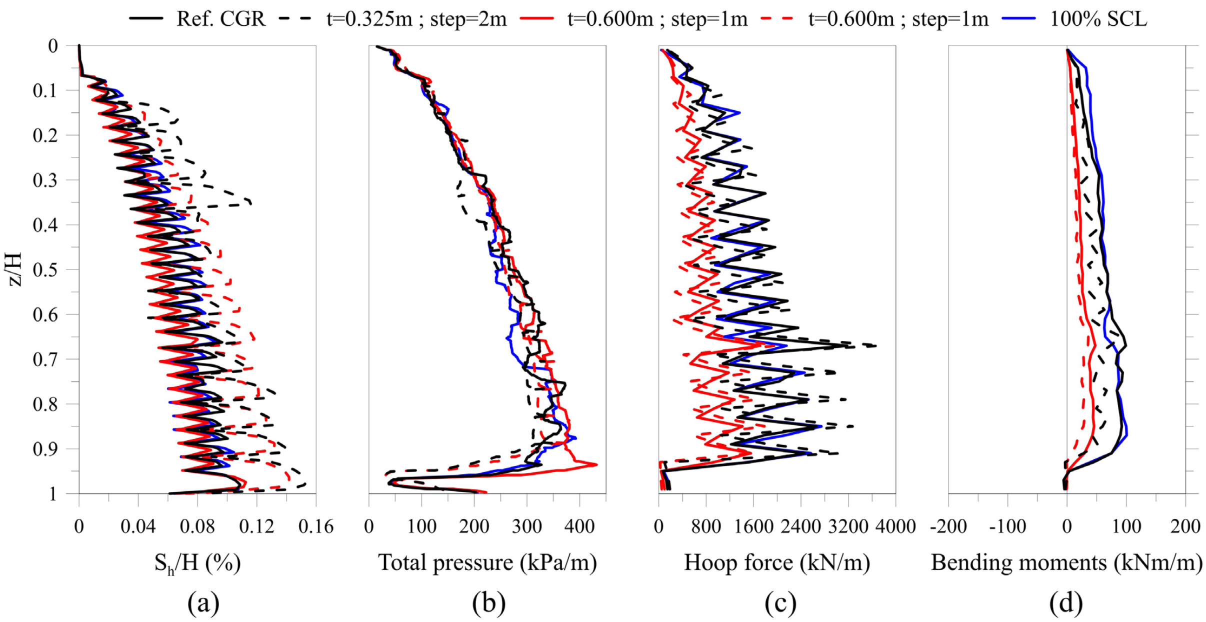

Figure 8. Influence of lining thickness and excavation step height on the lining in the EBS methodology: (a) horizontal displacement; (b) pressure; (c) hoop force; (d) bending moments.

observed for thicker linings. Increasing the excavation step height also slightly increases the hoop force values. Due to the construction process, the bending moments in the lining are small, not surpassing 100 kNm/m in the reference analysis, being even lower when thicker linings or greater excavation step heights are adopted. The analysis where PCS was replaced by SCL (100% SCL) provided very similar results to those of the reference analysis, indicating that the combination of the two materials has no significant impact on the overall shaft behavior.

3.2 SBE – Support Before Excavation

The thickness of the retaining structure and the length of the embedded wall are critical parameters in controlling ground movements and lining forces in deep excavations (Fernandes, 2015). To investigate the influence of these parameters on shaft construction, additional analyses were performed using the WCH shaft case as reference. In these analyses, the diaphragm wall thickness (*t*) was reduced by half to 0.75 m, and the embedded length (*L*) was reduced to 50 and 0%, with the latter simulating the absence of a wall beneath the excavation base.

Figure 9 shows that reducing the wall thickness has a considerable impact on settlements, with the maximum settlement increasing by about 75%, reaching 0.035%*H*. Reducing the embedded length to half has almost no impact on the settlements, while its complete removal originates a considerable increase in settlements between the wall and a distance of approximately 0.35*H* from its edge.

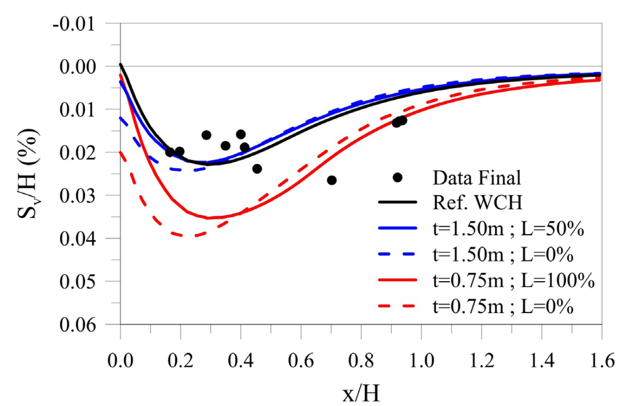

Figure 9. Influence of lining thickness and embedded length of the wall on settlements in the SBE methodology.

The results for the lining, presented in Figure 10, confirm the influence of the wall thickness on shaft behavior. With a thinner wall, larger lateral movements are observed, reaching a maximum in the middle part of the shaft of 0.12%*H* (a 50% increase). As a result, the total pressure decreases by about 25%, to approximately 150 kPa over the London Clay thickness. The reduction in lining forces is even greater, with the maximum hoop force observed in the middle part of the shaft decreasing from 3300 to 2250 kN/m (-32%), while the maximum absolute bending moment reduces from 1400 to just 430 kNm/m (-69%). In contrast, the embedded length appears to have a reduced impact, with slight reductions of about 5% in horizontal

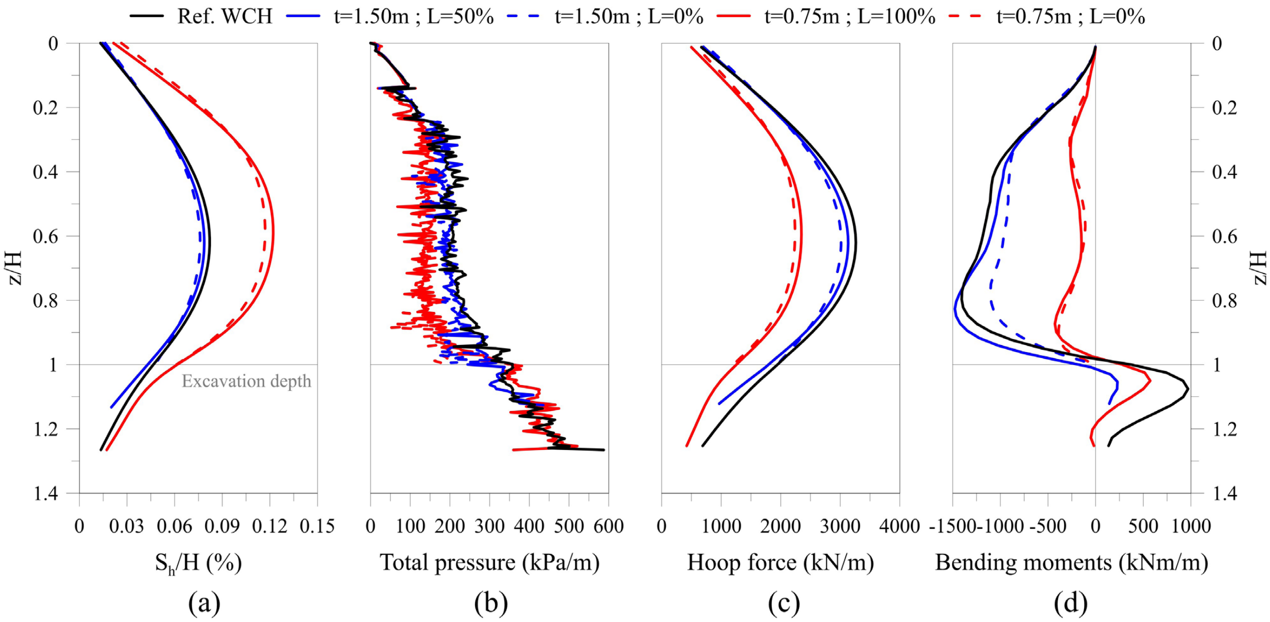

Figure 10. Influence of lining thickness and embedded length of the wall on settlements in the SBE methodology: (a) horizontal displacement; (b) pressure; (c) hoop force; (d) bending moments.

movements, 9% in the hoop force and 20% in the bending moment being observed. The reduced impact of the embedded length of the diaphragm wall is related to the auto-balanced circular shape of the shaft and the favorable mechanical properties of London Clay and Lambeth Group. However, as demonstrated by Fernandes (2015) the embedded length of the wall is fundamental not only for controlling ground movements but also for ensuring stability against base heave mechanisms. Therefore, its omission should not be considered without proper analysis.

3.3 DLS – Dual-Lined Shafts

In the case of the DLS methodology, one of the main aspects is related to the extent of SBE technique within the overall shaft height. A smaller SBE percentage implies that most of the shaft excavation follows the EBS approach, whereas a higher percentage resembles a behavior more similar to the SBE technique. Naturally, the extent of SBE is usually determined by ground conditions, as the pre-installed support system is essential for stabilizing less competent soils during the excavation. To assess the influence of the balance between these two different support systems, two additional analyses were carried out based on the KG case. Given that SBE accounts for 52% of the KG shaft, the two analyses considered SBE extents of 30% and 75%, with the former being conditioned by the thickness of the superficial deposits, which require prior support before excavation.

The settlements obtained from the analyses are presented in Figure 11 for the stages where the excavation reaches the tip of the piles (i.e. marking the end of the SBE technique and thus corresponding to a different depth for each of the three analyses shown) and for the final excavation. When the excavation reaches the tip of the piles, a slight heave is observed near the wall in all cases. At greater distances, minor settlements occur, which increase with the SBE percentage. This result is justified by the much deeper excavation level associated with a higher SBE extent. In contrast, the settlements observed for the final excavation stage increased considerably with the decrease in the SBE percentage. For 75% SBE, a maximum settlement of 0.033%H is determined, while for 30% SBE the settlement increased to approximately 0.115%H. Moreover, the shape of the settlement trough also varied considerably with the increase of the SBE percentage from a concave to a spandrel curve (Hsieh & Ou, 1998).

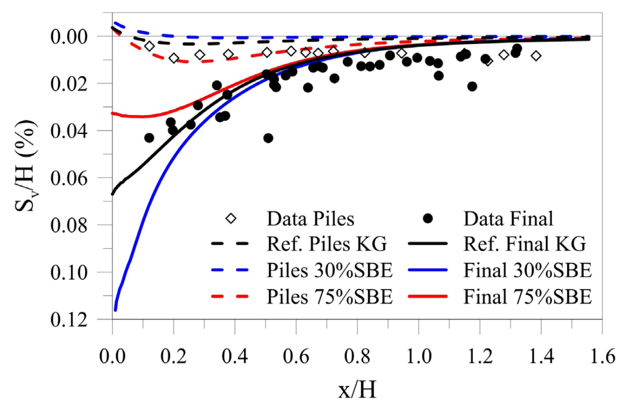

Figure 11. Influence of the percentage of SBE technique on settlements in the DLS methodology.

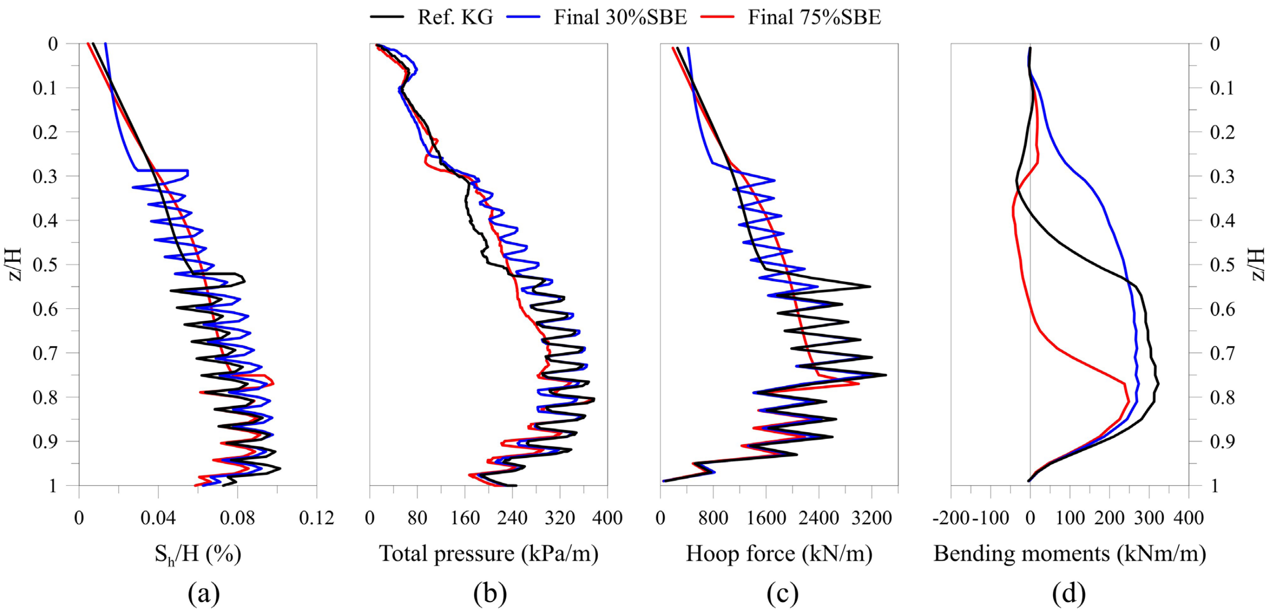

Figure 12. Influence of the percentage of SBE technique on settlements in the DLS methodology: (a) horizontal displacement; (b) pressure; (c) hoop force; (d) bending moments.

The lining results for the final excavation stage are presented in Figure 12 and show that increasing the percentage of SBE has a limited influence on the overall behavior of the lining. After transitioning from SBE to EBS, the lateral movements begin to fluctuate between the top and the base of the excavation steps, as occurred in the EBS study, but following a general trend comparable to that observed in the SBE extent. A similar trend is observed in total pressures and hoop forces, with a slight reduction as the SBE percentage increases. As for the bending moments, small values – within the same order of magnitude of those in EBS analyses – are predicted. The pressures and lining forces tend to increase with depth, reaching their maximum at about 75% of the total shaft height.

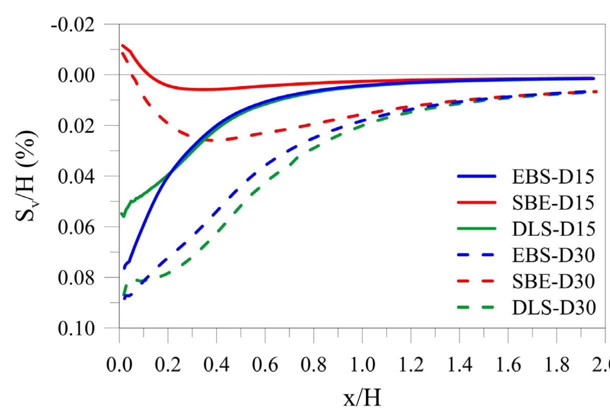

Figure 13. Settlements induced by different shaft methodologies.

4. Comparison of construction methodologies

This section presents a comparison of the different shaft construction methodologies. Due to its simplicity, the stratigraphy and ground conditions observed at CGR site were selected for this study. Since the analyzed shafts had different geometries, two idealized shafts were considered: both with an excavation depth of 30 m – consistent with the three case studies – but with diameters of 15 m (similar to CGR and KG) and 30 m (similar to WCH). To ensure a realistic comparison the lining characteristics from each case study were adopted, with minor adjustments to accommodate the idealized geometries. In total, six analyses were performed, two for each of the three construction methodologies, corresponding to the two shaft diameters.

The settlements predicted by the six analyses are displayed in Figure 13, with the results showing that a larger diameter corresponds to higher settlements, regardless of the construction method adopted. As expected, the smaller settlements – including slight heave near the wall – are predicted by the SBE methodology. The EBS and DLS techniques yield similar results, although EBS predicts higher settlements in the vicinity of the wall.

The lateral displacements of the wall are presented in Figure 14a and confirm that an increase in shaft diameter corresponds to greater displacements across all construction methodologies. In agreement with the settlement results, the smallest horizontal displacements occur with the SBE method, while the EBS and DLS techniques predict similar values for the smaller shaft. However, for the larger shaft, a different behavior between EBS and DLS is observed. In the upper part of the shaft, where the DLS method employs SBE, higher movements are observed, whereas in the lower part the opposite occurs, with EBS predicting greater horizontal

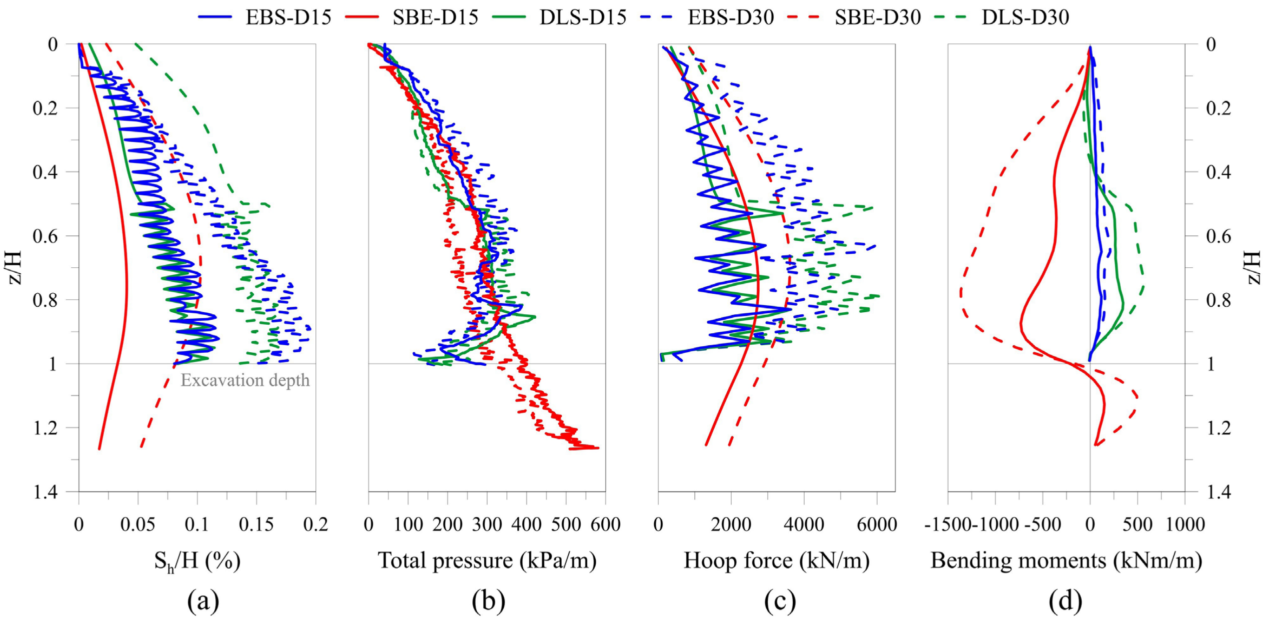

Figure 14. Lining results for different shaft methodologies: (a) horizontal displacement; (b) pressure; (c) hoop force; (d) bending moments.

displacements. The total pressure results in Figure 14b indicate that larger shafts experience lower pressures, with the differences being less pronounced, particularly in the SBE and DLS cases. All construction methods predict similar pressure distributions that increase with depth, though EBS presents slightly higher values throughout most of the shaft height, except near the base, where lower total pressures are observed due to soil decompression. The hoop forces exhibit a similar distribution with depth across all cases, with its maximum located at about 75% of the shaft height. The magnitude of the hoop forces increases considerably for the larger shaft, regardless of the construction methodology adopted (Figure 14c). Interestingly, for the smaller shaft, the hoop force predicted in the SBE method is greater than that observed in EBS and DLS, which yield identical results. In contrast, for the larger shaft, the opposite trend is observed, with SBE predicting smaller forces than EBS. The most significant differences in behavior are observed in the bending moments shown in Figure 14d, with the SBE analyses predicting considerably higher values. Moreover, the SBE cases indicate a curvature of the wall towards the interior of the excavation, while the opposite trend is observed in both the EBS and DLS methodologies. In agreement with the previous results, the larger shaft exhibits greater bending moments across all construction methods. However, it should be noted that in large shafts, the construction sequence of each excavation step is often divided into sections. As a result, arching develops not only in the vertical plane but also in the horizontal plane, contributing to the overall stability of the excavation. The use of 2D axisymmetric analysis cannot capture this construction sequence, leading to more conservative predictions as observed in the analyses.

5. Conclusions

This study evaluates the performance of three distinct construction methodologies, EBS, SBE and DLS, through extensive numerical analysis, which is validated against real case studies. The validation performed provided the following insights regarding the numerical modelling of each methodology:

- Incorporating hardening behavior in the lining is particularly important for the ESB methodology, improving the reproduction of available monitoring data.
- The method proposed by Schwamb & Soga (2015) simulates adequately the settlements induced by the wall installation.
- Lining stiffness anisotropy, caused by discontinuities between diaphragm wall panels or bored piles, has a considerable impact on shaft settlements, with the selection of the adequate stiffness anisotropy ratio still requiring further research.

The parametric studies provided the following insights regarding how some of the main variables inherent to each methodology influence shaft behavior:

- EBS – increasing the excavation step height and lining thickness leads to higher settlements due

to the greater unsupported soil length and to the additional weight of the lining, respectively, which are not compensated by the increased stiffness.
- SBE – the thickness of the wall is crucial for controlling ground movements, whereas the embedded length of the wall had a minor impact on the shaft behavior in the analyzed case, although it can be important in scenarios where less competent materials or higher water pressures are found.
- DLS – increasing the SBE percentage modifies the shaft behavior, making it closer to an EBS shaft excavation, with the settlement trough shifting from a concave to a spandrel shape.

The comparative study between all techniques led to the following conclusions:

- SBE induces the smallest ground movements but produces the highest lining forces.
- EBS exhibits the opposite, with higher ground movements due to soil decompression but lower lining forces.
- DLS methodology presents an intermediate behavior, although closer to EBS.
- The increase of shaft diameter translates into an increase of ground movements and lining forces, regardless of the shaft construction methodology.

The findings of this study provide valuable guidance into optimizing shaft design and selecting the appropriate construction methods, contributing to safer, more efficient and sustainable underground infrastructure development.

Acknowledgements

This work was partly financed by FCT / MCTES through national funds (PIDDAC) under the R&D Unit Institute for Sustainability and Innovation in Structural Engineering (ISISE), under reference UIDB / 04029/2020, and under the Associate Laboratory Advanced Production and Intelligent Systems ARISE under reference LA/P/0112/2020.

Declaration of interest

The authors have no conflicts of interest to declare. All co-authors have observed and affirmed the contents of the paper and there is no financial interest to report.

Authors' contributions

António M. G. Pedro: conceptualization, methodology, writing – original draft. David M. G. Taborda: conceptualization, data curation, methodology, software, writing – original draft. Lucas M. Repsold: investigation, validation, writing – review & editing. Jorge Almeida e Sousa: supervision, validation, writing – review & editing.

Data availability

The datasets generated and analyzed in the course of the current study are available from the corresponding author upon request.

Declaration of use of generative artificial intelligence

This work was prepared without the assistance of any generative artificial intelligence (GenAI) tools or services. All aspects of the manuscript were developed solely by the authors, who take full responsibility for the content of this publication.

List of symbols and abbreviations

c'	Effective cohesion
k_v	Vertical permeability
k_h	Horizontal permeability
p'_{ref}	Effective pressure of reference
s	Parameter controlling the effect of time on shotcrete stiffness
t	Lining thickness
t_{conc}	Age of sprayed concrete
y	Vertical coordinate on the model
y_{LC}	Coordinate of the top of the London Clay
x	Radial distance behind shaft wall
z	Depth
CGR	Channel Gate Road shaft
D	Shaft diameter
DLS	Dual-Lined Shafts
E	Young's modulus
E_{28}	Young's modulus of sprayed concrete at 28 days
E_z	Vertical stiffness
E_θ	Circumferential stiffness
EBS	Excavation Before Support
GWT	Ground Water Table
G_{ref}, m_G, a, b, $R_{g,min}$, G_{min}	Parameters for defining shear stiffness
H	Shaft depth
K_o	At-rest coefficient of earth pressure
K_{ref}, m_K, r, s, $R_{K,min}$, K_{min}	Parameters for defining bulk stiffness
KG	Kennington Green shaft
L	Embedded length of the lining
PCS	Pre-Cast Segments
S_v	Settlements
S_h	Horizontal displacements
SBE	Support Before Excavation
SCL	Sprayed Concrete Lining

WCH	Whitechapel Cambridge Heath shaft
WIP	Wished-in-place
γ	Unit weight
ν	Poisson's ratio
ϕ'	Angle of shearing resistance
ψ'	Angle of dilatancy

References

Admiraal, H., & Cornaro, A. (2016). Why underground space should be included in urban planning policy – And how this will enhance an urban underground future. *Tunnelling and Underground Space Technology*, 55, 214-220. http://doi.org/10.1016/j.tust.2015.11.013.

Bentley Systems. (2024). *PLAXIS2D 2024.2: reference manual.* Bentley Systems.

Bobylev, N. (2016). Underground space as an urban indicator: measuring use of subsurface. *Tunnelling and Underground Space Technology*, 55, 40-51. http://doi.org/10.1016/j.tust.2015.10.024.

Bui, T., Casarella, A., Di Donna, A., & Brinkgreve, R. (2019). Advanced thermo-hydro-mechanical modelling features for practical applications in energy geotechnics. In H. Sigursteinsson, S. Erlingsson & B. Bessason (Eds.), *Proceedings of the XVII European Conference on Soil Mechanics and Geotechnical Engineering*. The Icelandic Geotechnical Society.

Cabarkapa, Z., Milligan, G.W.E., Menkiti, C.O., Murphy, J., & Potts, D.M. (2003). Design and performance of a large diameter shaft in Dublin Boulder Clay. In T. Newson (Ed.), Proceedings of the BGA International Conference on Foundations: Innovations, observations, design and practice (pp. 175-185). London: Thomas Telford

Comité Euro-International du Béton & Fédération International de la Précontrainte – CEB-FIP. (1993). C*EB-FIP Model Code 1990*. Thomas Telford.

Crossrail Ltd. (2011). *Groundwater Level Monitoring – December 2011, Rev. 2.0* (Report no. CRL1-GCG-C2-RAN-CRG03-00002). Crossrail Ltd.

Debrock, S., Van Acker, M., & Admiraal, H. (2023). Design recommendations for sustainable urban underground spaces. *Tunnelling and Underground Space Technology*, 140, 1-15. http://doi.org/10.1016/j.tust.2023.105332.

Doig, P.J. (2012). Shaft construction for civil engineering projects. In *Proceedings of the 3rd International Conference on Shaft Design and Construction*. London: IOM3.

Falco, N., Bilotta, E., Divall, S., & Goodey, R.J. (2022). Numerical analysis of deep ground movements induced by circular shaft construction. In M. Rahman & M. Jaksa (Eds.), *Proceedings of the 20th International Conference on Soil Mechanics and Geotechnical Engineering*. Sidney: Australian Geomechanics Society.

Faustin, N.E., Elshafie, M.Z., & Mair, R.J. (2018). Case studies of circular shaft construction in London. *Geotechnical Engineering*, 171(5), 391-404. http://doi.org/10.1680/jgeen.17.00166.

Fernandes, M.M. (2015). New developments in the control and prediction of the movements induced by deep excavations in soft soils. *Soils and Rocks*, 38(3), 191-215. http://doi.org/10.28927/SR.383191.

Gawecka, K.A., Taborda, D.M.G., Potts, D.M., Cui, W., Zdravković, L., & Haji Kasri, M.S. (2017). Numerical modelling of thermo-active piles in London Clay. *Geotechnical Engineering*, 170(3), 201-219. http://doi.org/10.1680/jgeen.16.00096.

Gomes, A.T. (2008). *Elliptical shafts open by the sequential excavation method – Oporto Metro* [Doctoral thesis]. University of Porto.

Gourvenec, S.M., & Powrie, W. (1999). Three-dimensional finite-element analysis of diaphragm wall installation. *Geotechnique*, 49(6), 801-823. http://doi.org/10.1680/geot.1999.49.6.801.

Hsieh, P.G., & Ou, C.Y. (1998). Shape of ground surface settlement profiles caused by excavation. *Canadian Geotechnical Journal*, 35(6), 1004-1017. http://doi.org/10.1139/t98-056.

King, C. (1981). The stratigraphy of the London Clay and associated deposits. In W. Backhuys (Ed.), *Tertiary Research Special Paper* (Vol. 6). Tertiary Research Group.

Kuchler, M., Craig-Thompson, A., Alofe, E., & Tryggvason, A. (2024). SubCity: planning for a sustainable subsurface in Stockholm. *Tunnelling and Underground Space Technology*, 144, 105545. http://doi.org/10.1016/j.tust.2023.105545.

Le, B.T., Goodey, R.J., & Divall, S. (2019). Subsurface ground movements due to circular shaft construction. *Soil and Foundation*, 59(5), 1160-1171. http://doi.org/10.1016/j.sandf.2019.03.013.

Lin, D., Broere, W., & Cui, J. (2022). Underground space utilisation and new town development: Experiences, lessons and implications. *Tunnelling and Underground Space Technology*, 119, 104204. http://doi.org/10.1016/j.tust.2021.104204.

Lings, M.L., Ng, C.W.W., & Nash, D.F.T. (1994). The lateral pressure of wet concrete in diapragm wall pannels cast under bentonite. *Geotechnical Engineering*, 107(3), 163-172. http://doi.org/10.1680/igeng.1994.26469.

Muramatsu, M., & Abe, Y. (1996). Considerations in shaft excavation and peripheral ground deformation. In R.J. Mair & R.N. Taylor (Eds.), *Geotechnical aspects of underground construction in soft ground* (pp. 173-178). A. A. Balkema.

Pedro, A., Zdravković, L., Potts, D., & Almeida e Sousa, J. (2019). Numerical modelling of the Ivens shaft construction in Lisbon, Portugal. *Geotechnical Engineering*, 172(3), 263-282. http://doi.org/10.1680/jgeen.18.00080.

Pedro, A.M.G., Repsold, L., & Almeida e Sousa, J. (2024). Assessing the sustainability of alternative shaft construction methods. *Applied*, 14(11), 4476. http://doi.org/10.3390/app14114476.

Quigg, G. (2019). Battersea cable tunnel: powering regeneration in central London, UK. *Proceedings of the Institution of Civil Engineers. Civil Engineering*, 172(2), 77-82. http://doi.org/10.1680/jcien.18.00020.

Repsold, L., Pedro, A.M.G., & Almeida e Sousa, J. (2024). Numerical modelling of shafts – comparison between SBE and EBS construction methods. In N. Guerra, M.M. Fernandes, C. Ferreira, A.G. Correia, A. Pinto & P.S. Pinto (Eds.), *Geotechnical engineering challenges to meet current and emerging needs of society* (1st ed., pp. 2573-2576). CRC Press. http://doi.org/10.1201/9781003431749-498.

Royston, R., Sheil, B.B., & Byrne, W.B. (2022). Monitoring the construction of a large-diameter caisson in sand. *Proceedings of the Institution of Civil Engineers - Geotechnical Engineering*, 175(3), 323-339. http://doi.org/10.1680/jgeen.19.00266.

Sailer, E., Taborda, D.M., Zdravković, L., & Potts, D.M. (2019). Fundamentals of the coupled thermo-hydro-mechanical behaviour of thermo-active retaining walls. *Computers and Geotechnics*, 109, 189-203. http://doi.org/10.1016/j.compgeo.2019.01.017.

Schroeder, F., Potts, D., & Addenbrooke, T. (2004). The influence of pile group loading on existing tunnels. *Geotechnique*, 54(6), 351-362. http://doi.org/10.1680/geot.2004.54.6.351.

Schwamb, T., & Soga, K. (2015). Numerical modelling of a deep circular excavation at Abbey Mills in London. *Geotechnique*, 65(7), 604-619. http://doi.org/10.1680/geot.14.P.251.

Simpson, B., Blower, T., Craig, R., & Wilkinson, W. (1989). *The engineering implications of rising groundwater levels in the deep aquifer beneath London*. CIRIA.

Taborda, D.M.G., Potts, D.M., & Zdravković, L. (2016). On the assessment of energy dissipated through hysteresis in finite element analysis. *Computers and Geotechnics*, 71, 180-194. http://doi.org/10.1016/j.compgeo.2015.09.001.

Taborda, D.M.G., Kontoe, S., & Tsiampousi, A. (2023). IC MAGE Flow Model 01 – Nonlinearly Varying Anisotropic Permeability (Version 1.0). *Zenodo*. http://doi.org/10.5281/zenodo.7796383.

Taborda, D.M.G., Kontoe, S., & Tsiampousi, A. (2024a). IC MAGE Model 01 – Strain-Hardening/Softening Mohr-Coulomb Failure Criterion with Isotropic Small Strain Stiffness (Version 2.2). *Zenodo*. http://doi.org/10.5281/zenodo.13891265.

Taborda, D.M.G., Kontoe, S., & Tsiampousi, A. (2024b). IC MAGE UMIP – universal model interface for PLAXIS (Version 3.6). *Zenodo*. http://doi.org/10.5281/zenodo.13890543.

Taborda, D.M.G., Pedro, A.M.G., Kontoe, S., & Tsiampousi, A. (2025a). IC MAGE Model 07 – Simple non-linear time-dependent anisotropic stiffness model for concrete (Version 2.0). *Zenodo*. http://doi.org/10.5281/zenodo.14847116.

Taborda, D.M.G., Pedro, A.M.G., Xia, H., & Hardy, S. (2025b). A methodology for improved predictions of surface ground movements around shafts. *Geotechnical Engineering*, 178(4), 479-493. http://doi.org/10.1680/jgeen.24.00258.

Walton, G., Kim, E., Sinha, S., Sturgis, G., & Berberick, D. (2018). Investigation of shaft stability and anisotropic deformation in a deep shaft in Idaho, United States. *International Journal of Rock Mechanics and Mining Sciences*, 105, 160-171. http://doi.org/10.1016/j.ijrmms.2018.03.017.

Zdravkovic, L., Potts, D.M., & St John, H.D. (2005). Modelling of a 3D excavation in finite element analysis. *Geotechnique*, 55(7), 497-513. http://doi.org/10.1680/geot.2005.55.7.497.